PHYSICAL REVIEW A **96**, 061401(R) (2017)

Excitonlike exchange in two-photon transitions of pairs of cold Rb Rydberg atoms

Jeonghun Lee,* Phatthamon Kongkhambut, and T. F. Gallagher
Department of Physics, University of Virginia, Charlottesville, Virginia 22904-0714, USA
(Received 5 August 2017; published 26 December 2017)

We have observed an excitonlike exchange in two-photon microwave transitions between pairs of cold Rb Rydberg atoms, specifically, transitions in which a $ns_{1/2}ns_{1/2}$ pair undergoes the transition to the $np_{1/2}np_{3/2}$ and $np_{3/2}np_{1/2}$ states. This transition occurs due to the excitonlike $ns_{1/2}np_j \leftrightarrow np_jns_{1/2}$ exchange in the intermediate states, and the process can be thought of as a Förster resonant energy transfer between Floquet, or dressed, states. In addition, the measurements provide clear evidence of the importance of the three-dimensional nature of the dipole-dipole interaction.

DOI: 10.1103/PhysRevA.96.061401

Using the exaggerated properties of Rydberg atoms with cold atoms has proven to be most fruitful. For example, admixing a small amount of Rydberg character into ground-state atoms, often termed Rydberg dressing, endows the ground-state atoms with some of the strong dipole-dipole interactions of Rydberg atoms [1–3]. Cold Rydberg atoms themselves interact so strongly that at the temperature of the atoms in a magneto-optical trap (MOT), 100 μK, they are effectively frozen in place on the microsecond time scale of interest, opening many new avenues to explore. The use of cold, essentially stationary, Rydberg atoms has been explored for applications including quantum information [4–7], the production of exotic molecules [8–17], and the construction of an artificial solid [18–20]. Excellent summaries of cold Rydberg atom work can be found in recent reviews [21–23]. A recurring theme is excitation transport, in some cases as a Frenkel exciton. For example, Förster resonant energy transfer has been reported in many systems [24–28], and resonant energy transfer involving as many as four atoms has been observed [29,30]. Other forms of excitation transport have been explored both theoretically [31–34] and experimentally [35–38]. For example, dipole-dipole excitation transfer back and forth along a linear chain of atoms has been examined theoretically [31] and realized experimentally for a chain of three atoms [36].

Here, we report a different form of excitation transport, excitonlike transfer in two-photon microwave transitions of pairs of cold Rb Rydberg atoms. Specifically, we have observed transitions from $ns_{1/2}ns_{1/2}$ pairs to $np_{1/2}np_{3/2}$ and $np_{3/2}np_{1/2}$ pairs, at a frequency midway between the atomic $ns_{1/2} \rightarrow np_{1/2}$ and $ns_{1/2} \rightarrow np_{3/2}$ transition frequencies, as shown by Fig. 1. The observation of transitions of Na $3s_{1/2}3s_{1/2}$ pairs to $3p_{1/2}3p_{3/2}$ and $3p_{3/2}3p_{1/2}$ pairs has been reported, but in an entirely different regime [39]. The atoms were colliding, and the coupling could be treated perturbatively. In contrast, in these measurements the atoms are essentially stationary, and the coupling is too strong to be treated perturbatively. Our measurements are more similar to those done with molecules in a solid matrix [40]. Superficially similar is the observation of absorption features midway between Rydberg exciton states in Cu_2O, but the mechanism is different [41].

The resonant transition we observe cannot be driven in isolated atoms by a single frequency microwave field, only in pairs of atoms coupled by the dipole-dipole interaction. However, there is a small (<1%) nonresonant background due to the wings of the $ns_{1/2} \rightarrow np_j$ transitions in isolated atoms. Surprisingly, even with the dipole-dipole interaction some of the most obvious transitions, for example, those with no changes in the azimuthal angular momentum quantum number m_j of either atom, are not allowed due to cancellations of the interactions. Since the direction of the microwave field and the internuclear axis do not coincide, the dipole-dipole interaction does not conserve azimuthal angular momentum in the field direction. As a result, each of the four $ns_{1/2}ns_{1/2}$ levels is coupled to many of the 16 $np_{1/2}np_{3/2}$ and $np_{3/2}np_{1/2}$ levels, underscoring the importance of the inherently three-dimensional nature of the dipole-dipole interaction. In the following, we describe qualitatively how the transitions occur, outline the experimental approach, summarize our observations, and compare them to a model in which the transitions are described as Förster excitation transfers of Floquet, or dressed, states.

To understand the role of the dipole-dipole exchange in these two-photon transitions we consider a pair of closely spaced atoms, A and B, displaced from A by **R**. We construct molecular states which are ordered direct products of the states of the two atoms. For example, in the state $ns_{1/2}np_{1/2}$, atom A is in the $ns_{1/2}$ state, and atom B is in the $np_{1/2}$ state. The initial state of the microwave transition is the $ns_{1/2}ns_{1/2}$ state, which is excited by a pulsed laser. We drive the two-photon transition from the $ns_{1/2}ns_{1/2}$ state to the $np_{1/2}np_{3/2}$ and $np_{3/2}np_{1/2}$ states, via a virtual intermediate state, as shown by the dashed arrows in Fig. 1. There are four real intermediate states, $ns_{1/2}np_{1/2}$ and $np_{1/2}ns_{1/2}$, $ns_{1/2}np_{3/2}$ and $np_{3/2}ns_{1/2}$, and two final states, $np_{1/2}np_{3/2}$ and $np_{3/2}np_{1/2}$.

Why the transition of the pair cannot be driven in the absence of the dipole-dipole interaction is best shown by an example. In these transitions we assume that one atom undergoes the $ns_{1/2} \rightarrow np_j$ transition, while the other is a spectator [42,43]. For each path from $ns_{1/2}ns_{1/2}$ to $np_{1/2}np_{3/2}$ via the $np_{1/2}ns_{1/2}$ state there is a path through the $ns_{1/2}np_{3/2}$ state with the same dipole matrix elements and precisely opposite detuning, resulting in a vanishing two-photon matrix element. When the dipole-dipole interactions in the off-resonant intermediate states, shown by the double-headed arrows of Fig. 1, are taken into account, the transition is allowed.

*jl7rf@virginia.edu

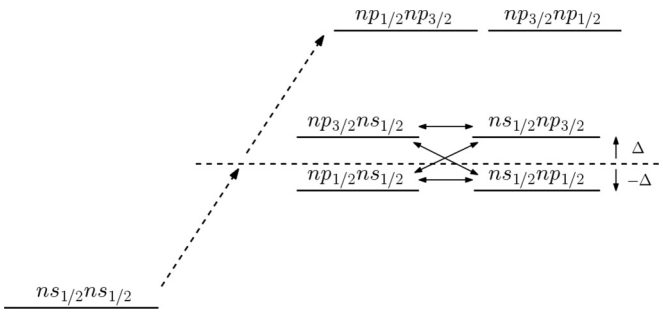

FIG. 1. Energy levels involved in the two-photon transition $ns_{1/2}ns_{1/2} \rightarrow np_{1/2}np_{3/2}, np_{3/2}np_{1/2}$. The real states are detuned from the virtual intermediate state by $\pm\Delta$.

A simplistic way of understanding the transition is that the dipole-dipole interaction in the intermediate states allows the two-photon transition to occur in one atom, as shown in Fig. 2.

The fact that the intermediate states are off resonant means that not only the dipole-dipole interactions of degenerate intermediate states, shown by the horizontal double-headed arrows of Fig. 1, but also those between nondegenerate states, shown by the slanted double-headed arrows, must be taken into account.

The experimental approach has been described previously, so our description here is brief [17,43]. ^{85}Rb atoms are trapped in a vapor-loaded magneto-optical trap (MOT), which is located at the center of a four-rod electrode structure and provides a steady population of Rb atoms in the $5p_{3/2}$ state. Atoms are excited to the $ns_{1/2}$ state by a 10-μJ, 10-ns, 150-MHz bandwidth, 480-nm laser pulse at a 20-Hz repetition rate. Subsequent to laser excitation, the atoms are exposed to a 1-μs-long microwave pulse to drive the two-photon transition shown in Fig. 1. After the end of the microwave pulse, a 3-μs rise-time field ionization pulse is applied to two of the rods, field ionizing the Rydberg atoms and driving the resulting ions to a microchannel plate (MCP) detector. Atoms which have undergone the transition to either np_j state are ionized earlier in the rising field pulse than atoms in the $ns_{1/2}$ state, and the time-resolved np_j signal is recorded with a gated integrator as the microwave frequency is slowly swept across the resonance over many shots of the pulsed laser.

The Rydberg atom density ρ has the following form, $\rho(x,y,z) = \rho_0 e^{-(x^2+y^2+z^2)/r_M^2} e^{-(x^2+y^2)/r_L^2}$, where $r_M = 0.3$ mm and $r_L = 0.2$ mm are the radii of the MOT and the 480-nm laser beam (propagating in the z direction), respectively; ρ_0 is the density at the center of the trap; and x, y, and z are the Cartesian displacements from the center of the trap. The maximum value of ρ_0 is 5×10^8 cm^{-3}, and the uncertainty in the absolute density measurement is a factor of 3.

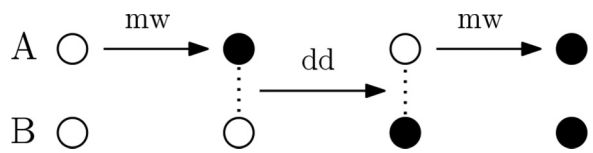

FIG. 2. Simple picture of the transition of two atoms A and B showing how the dipole-dipole interaction (dd) allows the microwave transition (mw) to occur in atom A only. ns atom (○), np atom (●).

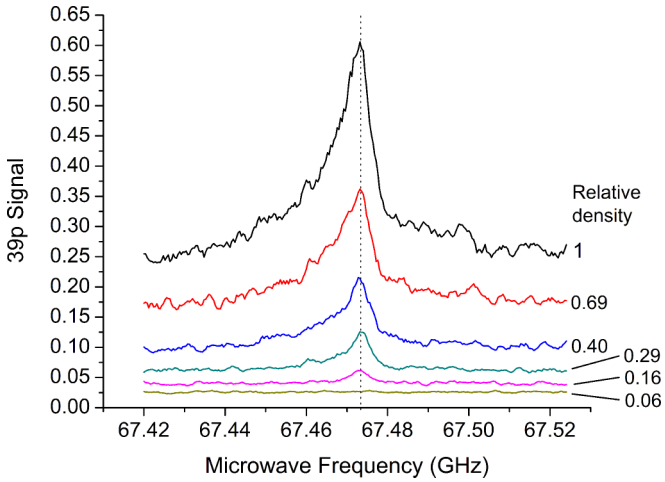

FIG. 3. Observed $39p$ signal vs microwave frequency at relative densities of 0.06–1. At relative density 1, $\rho_0 = 4.9 \times 10^8$ cm^{-3}. The microwave field amplitude is $E = 0.277$ V/cm, and the dotted line is at the $R = \infty$ microwave frequency of the two-photon $39s_{1/2}39s_{1/2}$-$39p_{1/2}39p_{3/2}/39p_{3/2}39p_{1/2}$ transition.

The microwaves are generated in an Agilent E8247C synthesizer, and a General Microwave DM862B switch is used to form the microwaves into 1-μs-long pulses. A Narda DBS2640X220 active doubler followed by a Pacific Millimeter V2WO passive doubler is used to generate microwaves in the 53–75 GHz range. The microwaves propagate from a horn outside the vacuum system to the atoms in the MOT volume. While the microwaves emanating from the horn are linearly polarized, scattering from the rods results in an elliptically polarized field [44]. The relative microwave field is controlled with a Millitech DRA-15 precision attenuator in the final waveguide, and the absolute microwave field is determined from the power broadening of single photon atomic $ns_{1/2} \rightarrow np_j$ transitions at low density.

We have observed the $ns_{1/2}ns_{1/2} \rightarrow np_{1/2}np_{3/2}/np_{3/2}np_{1/2}$ transition shown in Fig. 1 for both $n = 38$ and $n = 39$, and in Fig. 3 we show the observed $n = 39$ resonances for several Rydberg atom densities and a constant microwave field amplitude $E = 277$ mV/cm. At this field the $39s$-$39p_{1/2}$ atomic resonance is broadened to a full width at half maximum (FWHM) of ∼250 MHz. Several features are apparent in Fig. 3. First, the off-resonant background, due primarily to $39s_{1/2} \rightarrow 39p_j$ transitions driven by blackbody radiation [45,46], increases linearly with the Rydberg atom density. Second, as shown by the dotted line at 67.474 GHz, the frequency of the observed resonance matches half the $R = \infty$ $39s_{1/2}39s_{1/2}$-$39p_{1/2}39p_{3/2}$ zero-field interval of 134.948 GHz. Third, the amplitude of the resonance increases approximately quadratically with the density. This point is shown explicitly by Fig. 4, which shows that the fractional population transfer (FPT) increases linearly with the Rydberg atom density. FPT is defined as the fraction of the population which is resonantly transferred to the np_j states at the peak of the resonance, i.e., at 67.474 GHz in Fig. 3. At low density the resonance has a width of 5 MHz (FWHM), 10 MHz in the two-photon interval, due primarily to the trap B field inhomogeneity and impure microwave polarization [47]. At higher densities broadening

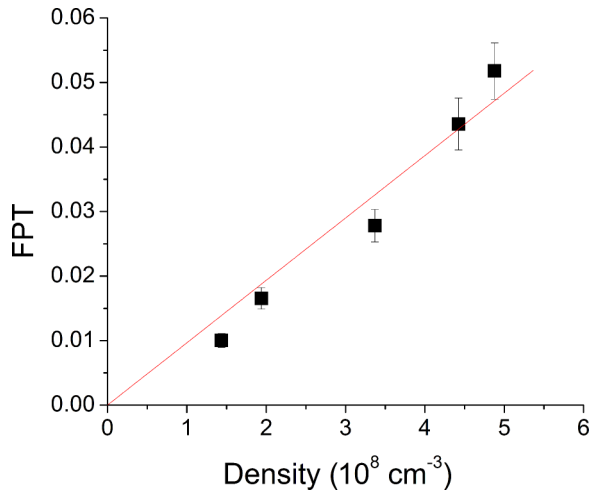

FIG. 4. Fractional population transfer (FPT) vs peak density ρ_0, with a microwave field amplitude 0.277 V/cm. The dashed line is a fit of the data to a line passing through the origin.

to 11 MHz (22 MHz in the two-photon interval) is observed, primarily due to a wing's developing on the low-frequency side of the resonance, which is not yet understood.

When the microwave field is varied, with the density held fixed, we observe a minimal frequency shift of the resonance, which is unexpected. Simple estimates on the basis of the levels shown in Fig. 1 suggest that shifts of up to 5 MHz should be observable. We attribute the lack of an evident shift to the presence of other coupled levels not shown in Fig. 1. More interesting from our present point of view, the FPT exhibits a quadratic dependence on the microwave electric field, as shown in Fig. 5. In sum, the FPT is quadratic in the microwave field amplitude and linear in the atomic density.

To understand the FPT quantitatively we have developed a model based on Förster resonance of Floquet, or dressed, states. At the resonance of Figs. 1 and 3 the $ns_{1/2}ns_{1/2}$ state is degenerate with the Floquet states $np_{1/2}np_{3/2}$ and $np_{3/2}np_{1/2}$ minus two microwave photons. We first compute

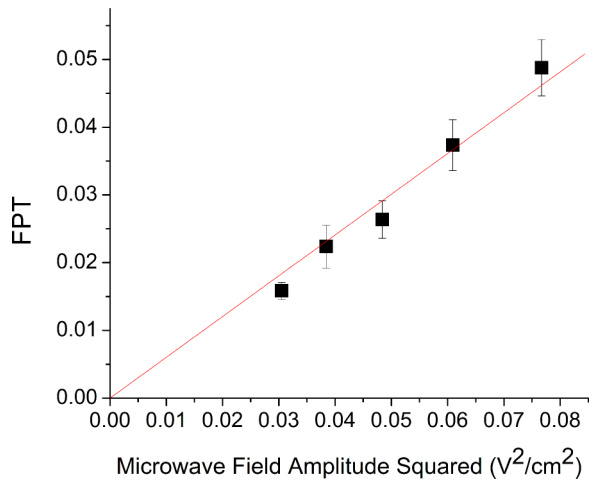

FIG. 5. Fractional population transfer (FPT) vs squared microwave field amplitude at peak density $\rho_0 = 4.2 \times 10^8$ cm^{-3}. The dashed line is a fit of the data to a line passing through the origin.

the probability for the transition from each $ns_{1/2}ns_{1/2}$ level to each of the $np_{1/2}np_{3/2}$ and $np_{3/2}np_{1/2}$ levels for fixed internuclear separation R and microwave field amplitude E. We then compute the average population transfer for one of these transitions at density ρ, and average over the density of Rydberg atoms in the trap. Finally, we multiply by the number of possible transitions to determine the FPT.

We begin by ignoring the dipole-dipole interaction and constructing Floquet states, in which integral numbers of microwave photons are added to or subtracted from the bare two-atom states [48]. For this problem the relevant Floquet states are those in which one photon is subtracted for each np_j atom. Examples of the Floquet states are $|ns_{1/2}ns_{1/2}\rangle$, $|ns_{1/2}np_{1/2}\rangle_{-1}$, and $|np_{1/2}np_{3/2}\rangle_{-2}$, where the subscripts indicate the number of photons subtracted. The microwave field can be written as $\mathbf{E}(t) = \hat{\mathbf{z}}E\cos\omega t$. We ignore the scattering of the microwave field from the rods. The effect of the microwave field is to admix the $|ns_{1/2}np_j\rangle_{-1}$ and $|np_jns_{1/2}\rangle_{-1}$ states into the $|ns_{1/2}ns_{1/2}\rangle$, $|np_{3/2}np_{1/2}\rangle_{-2}$, and $|np_{1/2}np_{3/2}\rangle_{-2}$ states. We choose the z axis as the axis of quantization, and since $\mathbf{R}$ is not parallel to $\hat{\mathbf{z}}$ we must take into account the magnetic sublevels of the two atoms [12]. Examples of the eigenstates in the presence of the field, computed perturbatively, using the rotating-wave approximation, are

$$\begin{aligned}\left|ns_{\frac12\frac12}ns_{\frac12\frac12}\right\rangle^E = \left|ns_{\frac12\frac12}ns_{\frac12\frac12}\right\rangle + \frac{z_3E}{2\Delta}\Big[\left|np_{\frac32\frac12}ns_{\frac12\frac12}\right\rangle_{-1} \\ + \left|ns_{\frac12\frac12}np_{\frac32\frac12}\right\rangle_{-1}\Big] - \frac{z_1E}{2\Delta}\Big[\left|np_{\frac12\frac12}ns_{\frac12\frac12}\right\rangle_{-1} \\ + \left|ns_{\frac12\frac12}np_{\frac12\frac12}\right\rangle_{-1}\Big],\end{aligned} \tag{1a}$$

$$\begin{aligned}\left|np_{\frac12\frac12}np_{\frac32-\frac12}\right\rangle^E_{-2} = \left|np_{\frac12\frac12}np_{\frac32-\frac12}\right\rangle_{-2} + \frac{z_1E}{2\Delta}\left|ns_{\frac12\frac12}np_{\frac32-\frac12}\right\rangle_{-1} \\ - \frac{z_3E}{2\Delta}\left|np_{\frac12\frac12}ns_{\frac12-\frac12}\right\rangle_{-1},\end{aligned} \tag{1b}$$

where Δ is the magnitude of the detuning from resonance, and we define the matrix elements z_{2j}, x_{2j}, and x_{33} by

$$\begin{aligned} z_{2j} &= \left\langle ns_{\frac12\frac12}\right| z \left|np_{j\frac12}\right\rangle, \\ x_{2j} &= \left\langle ns_{\frac12\frac12}\right| x \left|np_{j-\frac12}\right\rangle, \\ x_{33} &= \left\langle ns_{\frac12\frac12}\right| x \left|np_{\frac32\frac32}\right\rangle, \end{aligned} \tag{2}$$

where $j = 1/2$ or $3/2$. The eigenstates of Eq. (1) are coupled by the dipole-dipole interaction

$$V_{dd} = \frac{\mathbf{r}_A\cdot\mathbf{r}_B}{R^3} - \frac{3(\mathbf{r}_A\cdot\mathbf{R})(\mathbf{r}_B\cdot\mathbf{R})}{R^5}, \tag{3}$$

where $\mathbf{r}_A$ and $\mathbf{r}_B$ are the internal positions of the electrons in the two atoms. The coupling occurs through the microwave induced admixtures of Eqs. (1a) and (1b). For example,

$$\begin{aligned}\left\langle ns_{\frac12\frac12}ns_{\frac12\frac12}\right|^E V_{dd}\left|np_{\frac12\frac12}np_{\frac32-\frac12}\right\rangle^E_{-2} \\ = -\frac{3E^2\sin\theta\cos\theta}{4\Delta^2R^3}\Big[z_3^2x_3z_1 + z_1^2x_3z_3 + z_3^2x_3z_1 \\ - z_1^2x_3z_1\Big],\end{aligned} \tag{4}$$

where θ is the angle between $\mathbf{R}$ and $\hat{\mathbf{z}}$. An important point underscored by Eq. (4) is that the dipole-dipole interaction does not conserve the azimuthal angular momentum about the field direction [12]. Summing over the four terms in the square brackets of Eq. (4) and averaging over θ from 0 to $\pi/2$ yields

$$\Omega = \left| \left\langle ns_{\frac{1}{2}\frac{1}{2}} ns_{\frac{1}{2}\frac{1}{2}} \right|^{E} V_{dd} \left| np_{\frac{1}{2}\frac{1}{2}} np_{\frac{3}{2}-\frac{1}{2}} \right\rangle_{-2}^{E} \right|_{\theta}$$
$$= \frac{0.044 \langle ns| r |np\rangle^4 E^2}{4\Delta^2 R^3}, \quad (5)$$

where the factor 0.044 is from the angular factors of the z_{2j} and x_{2j} matrix elements and the average over θ, and the radial matrix element $\langle ns| r |np\rangle \cong n^2$ [49]. We have computed the matrix elements analogous to the one in Eq. (5) for all four initial levels and all 16 final levels, and the average is given by

$$\bar{\Omega} = \frac{0.020 n^8 E^2}{4\Delta^2 R^3}. \quad (6)$$

We note in passing that since $\Delta \propto 1/n^3$, $\bar{\Omega} \propto n^{14}$.

The transition probability from an initial $ns_{1/2}ns_{1/2}$ level to a final $np_{1/2}np_{3/2}$ or $np_{3/2}np_{1/2}$ level is given by $P_{R>R_T} = \sin^2(\bar{\Omega}T)$, where T is the microwave pulse duration [50]. We define $R_T = R$ such that $\bar{\Omega}T = \pi/2$. Explicitly,

$$R_T^3 = \frac{0.020 n^8 E^2 T}{2\Delta^2 \pi}. \quad (7)$$

For $R = R_T$ the transition probability is one, and for $R < R_T$ the average transition probability is $P_{R<R_T} = 1/2$ since the population oscillates back and forth between the initial and final states during the microwave pulse. For $R \gg R_T$ the transition probability is $P_{R>R_T} = (\bar{\Omega}T)^2$ [50]. Only for $R \gg R_T$ can this transition be described using perturbation theory. The perturbative character when $R \gg R_T$ is, however, masked by the integral over the trap volume.

For a Rydberg atom density ρ we define the average atomic spacing $R_{\mathrm{av},\rho}$ by $\rho = 3/4\pi R_{\mathrm{av},\rho}^3$, where $R_{\mathrm{av},\rho} > R_T$ in these experiments. The fraction of pairs with $R < R_T$ is $R_T^3/R_{\mathrm{av},\rho}^3$, and their contribution to the population transfer at density ρ is $= R_T^3/2R_{\mathrm{av},\rho}^3$. Using $P_{R>R_T} = (\bar{\Omega}T)^2$ and integrating from $R = R_T$ to $R = R_{\mathrm{av},\rho}$ with the assumption that $R_{\mathrm{av},\rho} \gg R_T$ yields a contribution to the population transfer of $\pi^2 R_T^3/4R_{\mathrm{av},\rho}^3 \cong 5R_T^3/2R_{\mathrm{av},\rho}^3$, so at density ρ, the population transfer is $X_\rho^1 \cong 3R_T^3/R_{\mathrm{av},\rho}^3$, where the superscript one is a reminder that this is the population transfer due to one of the 16 possible transitions. Averaging over the trap density and accounting for inhomogeneous broadening leads to the result

$$X^1 \cong \frac{1.06 R_T^3}{R_{\mathrm{av},0}^3 T\Gamma}, \quad (8)$$

where $R_{\mathrm{av},0}$ is the average spacing at the peak density in the center of the trap, and the factor $T\Gamma$ accounts for the inhomogeneous broadening of $\Gamma = 10$ MHz. The density and microwave field scalings of Eq. (8) match those shown in Figs. 4 and 5. The scaling of Eq. (8) is valid for $R_{\mathrm{av},0}^3 > R_T^3$, a condition which is easily met in these experiments.

We have at this point determined the average transition probability for one of the 16 possible transitions from the $|ns_{1/2}ns_{1/2}\rangle$ to the $|np_{1/2}np_{3/2}\rangle$ and $|np_{3/2}np_{1/2}\rangle$ states. Multiplying this result by the number of final levels, 16, gives the expected FPT X, given by

$$X \cong \frac{17.0 R_T^3}{R_{\mathrm{av},0}^3 T\Gamma}. \quad (9)$$

We can compare the FPT given by the model to that observed in the experiment for $n = 39$. From the power broadening of the atomic $39s_{1/2}$-$39p_j$ transitions we estimate that for the data shown in Fig. 4, $n^2 E = 540$ MHz. Combining this value with $\Delta = 905$ MHz, and $T = 1$ μs (4.13×10^{10} a.u.) yields $R_T^3 = 1.08 \times 10^{14} a_0^3$. At the density $\rho_0 = 5 \times 10^8$ cm^{-3}, $R_{\mathrm{av},0}^3 = 3.2 \times 10^{15} a_0^3$. With $T\Gamma = 10$ we obtain $\mathcal{T} = 0.056$ at $\rho_0 = 5 \times 10^8$ cm^{-3}. This value is in good, probably fortuitous, agreement with the data of Fig. 4.

In conclusion, we have observed an unusual example of dipole-dipole excitation transport, one in which allows a two-photon transition forbidden in isolated atoms. Furthermore, it underscores the inherently three-dimensional nature of the dipole-dipole interaction; a one-dimensional model fails to reproduce the experimental results.

We acknowledge illuminating discussions with R. R. Jones, P. Pillet, C. A. Sackett, and S. Scheel. This work has been supported by the Air Force Office of Scientific Research under Grant No. FA9550-14-1-0288. P.K. would like to thank the Development and Promotion of Science and Technology Talents Project (DPST), Thailand for support.

[1] M. L. Wall, F. Robicheaux, and R. R. Jones, J. Phys. B **40**, 3693 (2007).

[2] G. Pupillo, A. Micheli, M. Boninsegni, I. Lesanovsky, and P. Zoller, Phys. Rev. Lett. **104**, 223002 (2010).

[3] C. Gaul, B. J. DeSalvo, J. A. Aman, F. B. Dunning, T. C. Killian, and T. Pohl, Phys. Rev. Lett. **116**, 243001 (2016).

[4] M. D. Lukin, M. Fleischhauer, R. Cote, L. M. Duan, D. Jaksch, J. I. Cirac, and P. Zoller, Phys. Rev. Lett. **87**, 037901 (2001).

[5] D. Moller, L. B. Madsen, and K. Molmer, Phys. Rev. Lett. **100**, 170504 (2008).

[6] M. Saffman, T. G. Walker, and K. Molmer, Rev. Mod. Phys. **82**, 2313 (2010).

[7] I. I. Beterov, M. Saffman, E. A. Yakshina, D. B. Tretyakov, V. M. Entin, S. Bergamini, E. A. Kuznetsova, and I. I. Ryabtsev, Phys. Rev. A **94**, 062307 (2016).

[8] C. H. Greene, A. S. Dickinson, and H. R. Sadeghpour, Phys. Rev. Lett. **85**, 2458 (2000).

[9] V. Bendkowsky, B. Butscher, J. Nipper, J. P. Shaffer, R. Low, and T. Pfau, Nature (London) **458**, 1005 (2009)

[10] J. Tallant, S. T. Rittenhouse, D. Booth, H. R. Sadeghpour, and J. P. Shaffer, Phys. Rev. Lett. **109**, 173202 (2012).

[11] C. Boisseau, I. Simbotin, and R. Cote, Phys. Rev. Lett. **88**, 133004 (2002).

[12] M. Kiffner, H. Park, W. Li, and T. F. Gallagher, Phys. Rev. A **86**, 031401 (2012).
[13] K. R. Overstreet, A. Schwettmann, J. Tallant, D. Booth, and J. P. Shaffer, Nat. Phys. **5**, 581 (2009).
[14] H. Saßmannshausen and J. Deiglmayr, Phys. Rev. Lett. **117**, 083401 (2016).
[15] H. Saßmannshausen, F. Merkt, and J. Deiglmayr, Phys. Rev. A **92**, 032505 (2015).
[16] Y. Yu, H. Park, and T. F. Gallagher, Phys. Rev. Lett. **111**, 173001 (2013).
[17] J. Lee and T. F. Gallagher, Phys. Rev. A **93**, 062509 (2016).
[18] H. Weimer, R. Low, T. Pfau, and H. P. Buchler, Phys. Rev. Lett. **101**, 250601 (2008).
[19] P. Schauß, M. Cheneau, M. Endres, T. Fukahara, S. Hild, A. Omran, T. Pohl, C. Gross, S. Kuhr, and I. Bloch, Nature (London) **491**, 87 (2012).
[20] N. Thaicharoen, A. Schwarzkopf, and G. Raithel, Phys. Rev. Lett. **118**, 133401 (2017).
[21] R. Low, H Weimer, J. Nipper, J. B. Balewski, B. Butscher, H. P. Buchler, and T. Pfau, J. Phys. B **45**, 113001 (2012).
[22] A. Browaeys, D. Barredo, and T. Lahaye, J. Phys. B **49**, 152001 (2016).
[23] J. Lim, H. Lee, and J. Ahn, J. Korean Phys. Soc. **63**, 867 (2013).
[24] I. Mourachko, D. Comparat, F. de Tomasi, A. Fioretti, P. Nosbaum, V. M. Akulin, and P. Pillet, Phys. Rev. Lett. **80**, 253 (1998).
[25] W. R. Anderson, J. R. Veale, and T. F. Gallagher, Phys. Rev. Lett. **80**, 249 (1998).
[26] M. R. Kutteruf and R. R. Jones, Phys. Rev. Lett. **108**, 013001 (2012).
[27] T. J. Carroll, K. Claringbould, A. Goodsell, M. J. Lim, and M. W. Noel, Phys. Rev. Lett. **93**, 153001 (2004).
[28] P. Bohlouli-Zanjani, J. A. Petrus, and J. D. D. Martin, Phys. Rev. Lett. **98**, 203005 (2007).
[29] J. H. Gurian, P. Cheinet, P. Huillery, A. Fioretti, J. Zhao, P. L. Gould, D. Comparat, and P. Pillet, Phys. Rev. Lett. **108**, 023005 (2012).
[30] R. Faoro, B. Pelle, A. Zuliani, P. Cheinet, E. Arimondo, and P. Pillet, Nat. Commun. **6**, 8173 (2015).
[31] S. Wuster, C. Ates, A. Eisfeld, and J. M. Rost, Phys. Rev. Lett. **105**, 053004 (2010).
[32] T. Scholak, T. Wellens, and A. Buchleitner, Phys. Rev. A **90**, 063415 (2014).
[33] S. Bettelli, D. Maxwell, T. Fernholz, C. S. Adams, I. Lesanovsky, and C. Ates, Phys. Rev. A **88**, 043436 (2013).
[34] D. W. Schonleber, A. Eisfeld, M. Genkin, S. Whitlock, and S. Wuster, Phys. Rev. Lett. **114**, 123005 (2015).
[35] C. S. E. van Ditzhuijzen, A. F. Koenderink, J. V. Hernandez, F. Robicheaux, L. D. Noordam, and H. B. van Linden van den Heuvell, Phys. Rev. Lett. **100**, 243201 (2008).
[36] D. Barredo, H. Labuhn, S. Ravets, T. Lahaye, A. Browaeys, and C. S. Adams, Phys. Rev. Lett. **114**, 113002 (2015).
[37] T. Zhou, S. Li, and R. R. Jones, Phys. Rev. A **89**, 063413 (2014).
[38] G. Gunter, H. Schempp, M. Robert-de-Saint-Vincent, V. Gavryusev, S. Helmrich, C. S. Hofmann, S. Whitlock, and M. Weidemuller, Science **342**, 954 (2013).
[39] E. Pedrozo-Penafiel, R. R. Paiva, F. J. Vivanco, V. S. Bagnato, and K. M. Farias, Phys. Rev. Lett. **108**, 253004 (2012).
[40] C. Hettich, C. Schmitt, J. Zitzmann, S. Kuhn, I. Gerhardt, and V. Sandoghar, Science **298**, 385 (2002).
[41] P. Grunwald, M. Aßmann, J. Heckotter, D. Frohlich, M. Bayer, H. Stolz, and S. Scheel, Phys. Rev. Lett. **117**, 133003 (2016).
[42] W. E. Cooke, T. F. Gallagher, S. A. Edelstein, and R. M. Hill, Phys. Rev. Lett. **40**, 178 (1978).
[43] H. Park, P. J. Tanner, B. J. Claessens, E. S. Shuman, and T. F. Gallagher, Phys. Rev. A **84**, 022704 (2011).
[44] L. Levac, M. S. thesis, University of Virginia, 2013.
[45] W. E. Cooke and T. F. Gallagher, Phys. Rev. A **21**, 588 (1980).
[46] T. F. Gallagher, *Rydberg Atoms* (Cambridge University Press, Cambridge, UK, 1996).
[47] H. Park, Ph.D. thesis, University of Virginia, 2012.
[48] J. H. Shirley, Phys. Rev. **138**, B979 (1965).
[49] T. G. Walker and M. Saffman, Phys. Rev. A **77**, 032723 (2008).
[50] P. Pillet, R. Kachru, N. H. Tran, W. W. Smith, and T. F. Gallagher, Phys. Rev. A **36**, 1132 (1987).